

# Improving performance and accuracy of 3D Kirchhoff migration

Herman Jaramillo\*. Geotrace Technologies

## SUMMARY

Since 3D Prestack Kirchhoff Depth Migration (KPSDM) has become one of the leading imaging tools for hydrocarbon exploration, its accurate and precise handling of the kinematical and dynamical aspects of the wavefield have become center stage to the R&D efforts worldwide. In a separate paper in this proceeding by the same author, describe a modified antialiasing filter weight that corrects for amplitude artifacts observable in earlier designs. Here we continue the efforts of developing an efficient true amplitude migration algorithm by suggesting a simplification of the traditional filtering done during this process that will improve the performance and precision of the results.

In most Kirchhoff migration implementations, a triangular smoothing filter is used to avoid high frequency aliasing along the migration operator. This filter is implemented in three steps: causal integration, anti-causal integration, and Laplace-type differentiation along the diffraction stacking surface. In addition a derivative filter (known as  $\rho$ -filter) is applied to the input data to correct for the wavelet phase rotation introduced by the Kirchhoff summation. We will find that the standard filtering sequence of applying the  $\rho$ -filter, causal integration, and anti-causal integration can be replaced by just an anti-causal integration. We will see how this simplification provides advantages in performance and accuracy.

## INTRODUCTION

Kirchhoff migration provides one of the best imaging solutions when data are non-uniformly distributed in space. It also is fast and flexible when it comes to input/output geometries. In our quest to make 3D KPSDM better and faster we have found an alternative to achieve a comparable result by replacing the traditional filtering sequence made of a  $\rho$ -filter, causal integration and anti-causal integration with a single anti-causal integration filter. Note that this is applicable to time as well as depth migration algorithms.

Before the data are stacked along a diffraction surface, they are filtered for waveform phase shaping and pre-filtered in preparation for the antialiasing operation applied during summation. Since the integration process shifts the waveform shape, the  $\rho$ -filter works restoring it. The anti-aliasing filter is applied in three stages: causal integration, anti-causal integration and then a Laplacian computation rolling along the stacking diffraction surface. By replacing these three filters by an anti-causal integration the performance and accuracy of the algorithm can be greatly improved. The results presented here also incorporate the normalization factor in the anti-aliasing filter mentioned above and described elsewhere in these proceedings. These corrections eliminate azimuthally anisotropic amplitude behavior on the migration impulse response as well as amplitude distortions with time and offset, introduced by the traditional scaling factor in Lumley et al. (1994) and Abma et al. (1999).

## THREE FILTERS IN ONE

Differentiation in the frequency domain can be accomplished by a multiplication by  $-i\omega$ , where  $\omega$  represents the circular frequency, and  $\Delta t$  is the temporal sampling rate. Let us define  $D$  as

$$D = -i\omega. \quad (1)$$

The discrete causal integrator is given by

$$I = \frac{1}{1-z} \Delta t \quad (2)$$

where  $z = e^{i\omega\Delta t}$ . Expanding  $z$  in its Taylor series we get, to first order,

$$z = e^{i\omega\Delta t} \approx 1 + i\omega\Delta t \quad (3)$$

so that

$$1 - z \approx -i\omega\Delta t. \quad (4)$$

The composition of the differentiation  $D$  and the causal integration  $I$ , up to leading order, is the identity. That is

$$ID \approx 1. \quad (5)$$

As the sampling rate  $\Delta t$  goes to zero the approximation becomes an equality. From this it is straightforward to conclude that the three filters:  $\rho$ -filter, causal integration and anti-causal integration should be equivalent to just an anti-causal integration. The numerical examples below confirms this statement.

Before showing the numerical examples, let us state that the  $\rho$ -filter could be applied directly in the time domain by convolving each input trace with a finite difference derivative operator. An accurate implementation of this filter would require many filter coefficients and would be relatively more expensive that the frequency domain implementation. The simplification that we propose does not apply when the  $\rho$ -filter is implemented in the time domain.

Figure 1 shows a synthetic trace with three zero phase wavelets, Figure 2 shows the trace after the three filters:  $\rho$ -filter, causal integration and anti-causal integration has been applied, Figure 3 shows the trace after only the anti-causal integration filter was applied. The traces in Figure 2 and Figure 3 are highly similar. However the amplitude level is different. The reason for the difference in amplitude is carefully studied in the companion paper in these proceedings.

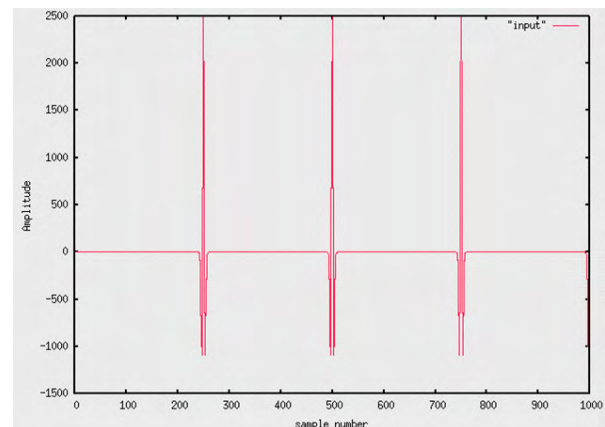


Figure 1: A synthetic trace with zero phase waveforms.

Figure 4 shows an example from a field trace. Here the upper trace is produced by the composition of the three filters:  $\rho$ -filter, causal integration and anti-causal integration, while the lower trace is obtained

## Improving performance and accuracy of 3D Kirchhoff migration

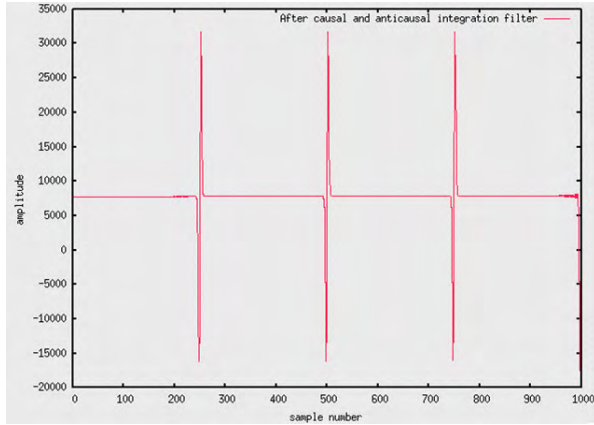


Figure 2: The trace in Figure 1, after application of the three filters:  $\rho$ -filter, causal integration and anti-causal integration.

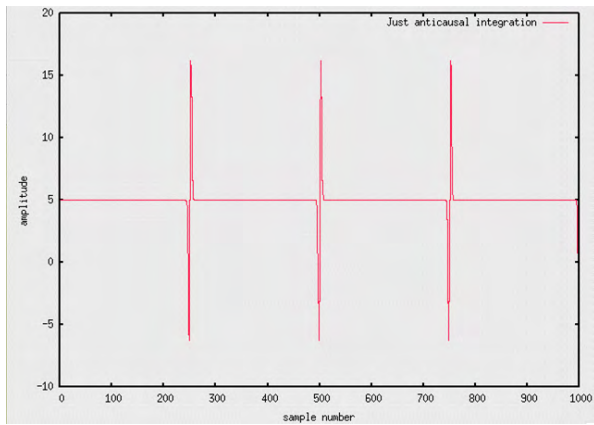


Figure 3: Trace after only the anti-causal integration filter was applied. Compare with figure (2). Note the amplitude values.

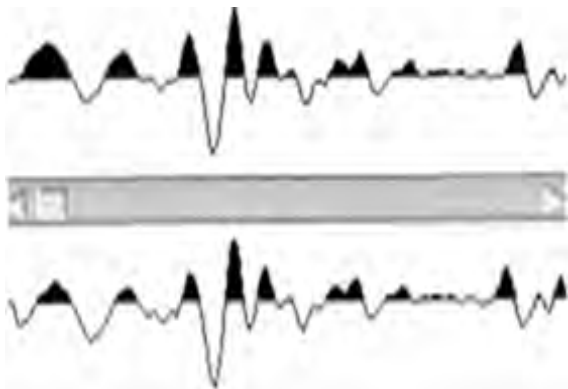


Figure 4: Top: A field data trace after application of the composition of  $\rho$ -filter, causal integration and anti-causal integration. Bottom: after anti-causal integration alone.

by applying the proposed anti-causal integration filter. We observe that both traces look very much alike. Let's examine the amplitude and phase responses from the two sets of filters and compare their responses. Figure 5 shows a piece of waveform of a migration impulse response using an algorithm that employs the three filters:  $\rho$ -filter, causal integration and anti-causal integration. It shows also the amplitude and phase spectra of the waveform. Figure 6 shows the corresponding amplitude and phase spectrum when only the anti-causal integration filter is used. It is clear from Figure 5 and 6 that the theoretical ideal phase of -90 degrees in the waveform spectrum, is more closely reproduced throughout the spectrum, when just an anti-causal integration filter is applied. It is also obvious that when only the anti-causal integration filter is applied in the migration algorithm, the amplitude spectrum is richer in high frequencies. The phase spectrum behavior in Figure 5 is due to the fact that the  $\rho$ -filter is applied in the frequency domain, after tapering the low and high frequencies to avoid artifacts in the time domain. While the three filters:  $\rho$ , causal and anti-causal integration are applied in the frequency domain, the anti-causal integration is easily applied in the time domain (as an accumulator from the end to the beginning of the trace). The fact that

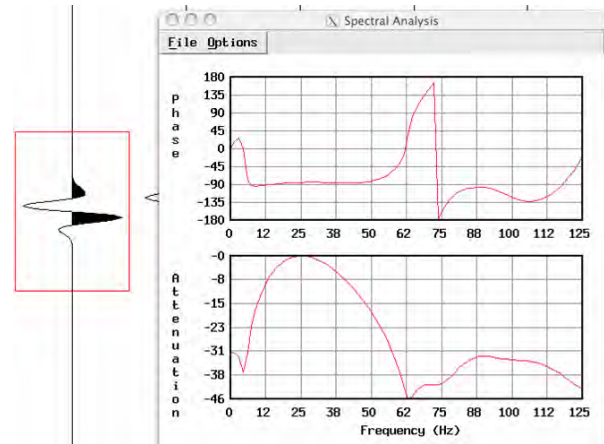


Figure 5: Amplitude and phase spectra of the waveform on the left, obtained from an impulse response of Kirchhoff migration using a

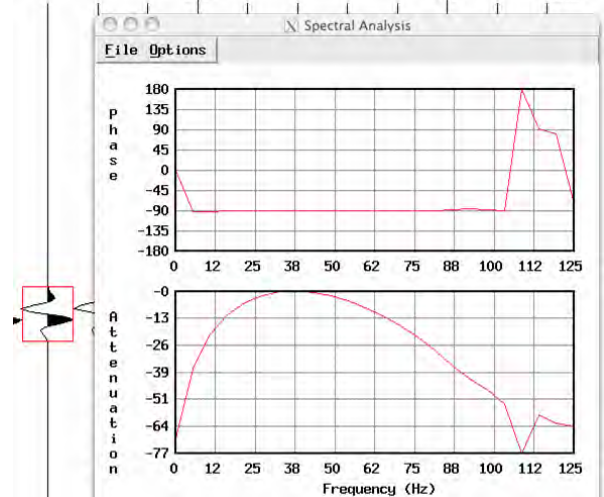


Figure 6: Amplitude and phase spectra of the waveform on the left, obtained after an impulse response of Kirchhoff migration using just an anti-causal integration

the anti-causal integration is done in the time domain, results not just in computational savings (no more Fast Fourier Transforms) but also

## Improving performance and accuracy of 3D Kirchhoff migration

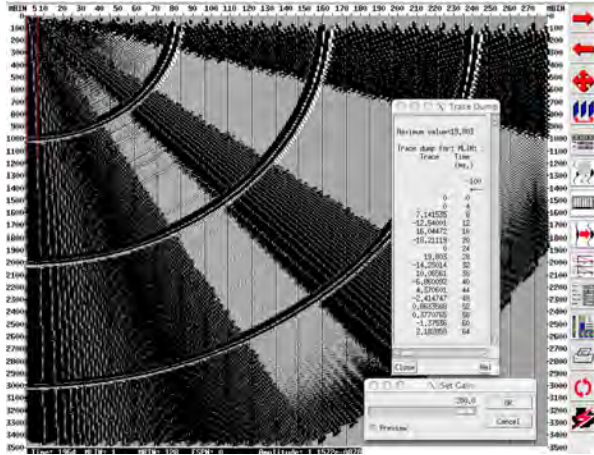


Figure 7: Kirchhoff migration impulse response using the three-filter cascade approach (displayed with a huge gain 200 db) show the presence of the beams of noise associated with frequency domain artifacts of the cascaded filters (wraparound).

in a better frequency response and lack of wraparound noises, so pervasive in frequency domain implementations. This is clearly visible in figures below where Kirchhoff impulse responses are displayed with the three-filter Figures 7 and with simply the anti-causal filter Figures 8. The beams of noise (only seen when the amplitude is gained to 200 decibels in Figures 7) are wraparound artifacts associated with the frequency domain method. On the other hand, Figure 8 shows none of this noises (even at this amplification) because of the time-domain implementation of the anti-causal integration. Given that no transformation in/out of the frequency domain (Fast Fourier Transforms) is required for the application of the anti-causal integration filter, a substantial savings in computer time has been observed. On a reasonable size migration the observed performance improvement was about 3:2 when compared to the traditional three-filter implementation.

### FIELD DATA EXAMPLE

Figure 9 shows a migration of a common offset section where the three filter methodology was applied, i.e.  $\rho$ -filter, causal integration and anti-causal integration. Figure 10 shows the corresponding migrated output using only anti-causal integration. Very little difference can be observed between these two sections demonstrating that the application of just the anti-causal integration should suffice. The performance gains more than justify the imperceptible differences in these sections making the application of the single anti-causal integration a preferred method over the three-step filtering traditionally used where  $\rho$ -filter, causal integration and anti-causal integration are applied in sequence.

### CONCLUSIONS

Traditionally, Kirchhoff migration is performed with the cascade of filters in order to correct for the phase rotation introduced by the integration process as well as for aliasing due to spatial and temporal sampling. The filters are the  $\rho$ -filter, causal integration and anti-causal integration. This paper provides a simplification of the 3D Kirchhoff migration algorithm by collapsing these three filters into just one anti-causal integration. The benefits of this substitution are: shorter processing times and cleaner (phase and amplitudes) results.

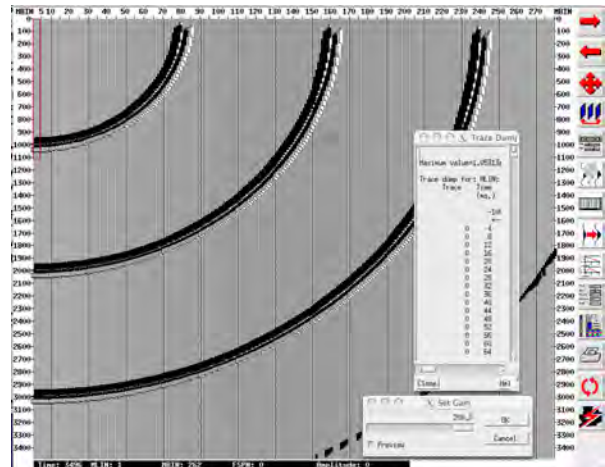


Figure 8: Kirchhoff migration impulse response using the single anti-causal filter (displayed with a huge gain 200 db) show no beams of noise. This is because computations (anti-causal integration) was performed in the time domain.

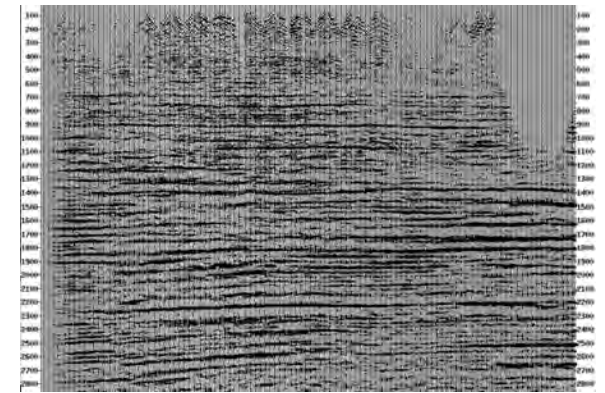


Figure 9: Migration of a common offset section, using the three filters:  $\rho$ -filter, causal integration and anti-causal integration

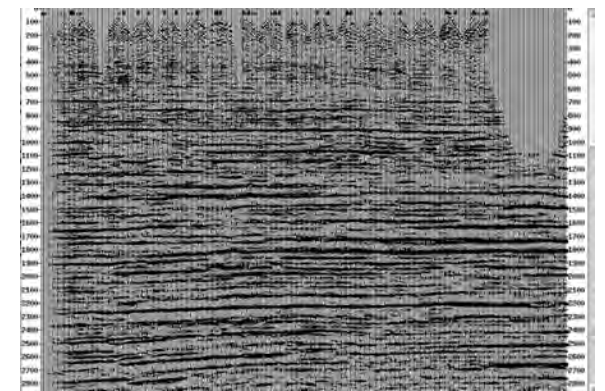


Figure 10: Migration corresponding to that of Figure 9 but this time only an anti-causal integration filter was applied.

## Improving performance and accuracy of 3D Kirchhoff migration

### ACKNOWLEDGMENTS

This research was conducted while the author was employed at Geo-Center, Inc. The field data set example was provided by Explora Seismic Processing Inc. Marcia Turner addressed some problems that motivated this research. I thank John Stevens, Plácido Mora and Gabriel Pérez, for helpful comments on the subject. Geotrace Technologies provided time and resources to prepare this manuscript.



[www.geotrace.com](http://www.geotrace.com)

GEOHUBS IN HOUSTON, DALLAS, LONDON AND CAIRO  
OFFICES WORLDWIDE